Article

Water-Assisted Perovskite Quantum Dots with High Optical Properties

Masaaki Yokoyama [1], Ryota Sato [1], Junya Enomoto [1], Naoaki Oshita [1], Taisei Kimura [1], Keisuke Kikuchi [1], Satoshi Asakura [2], Kazuki Umemoto [1] and Akito Masuhara [1,3,*]

1   Graduate School of Science and Engineering, Yamagata University, 4-3-16 Jonan Yonezawa, Yamagata 992-8510, Japan; tha54987@st.yamagata-u.ac.jp (M.Y.); t211431d@st.yamagata-u.ac.jp (R.S.); tya44954@st.yamagata-u.ac.jp (J.E.); t211813m@st.yamagata-u.ac.jp (N.O.); t211439m@st.yamagata-u.ac.jp (T.K.); t211060m@st.yamagata-u.ac.jp (K.K.); umemoto@yz.yamagata-u.ac.jp (K.U.)
2   Ise Chemicals Corporation, 1-3-1 Kyobashi, Tokyo 104-0031, Japan; asakura@isechem.co.jp
3   Frontier Center for Organic Materials (FROM), Yamagata University, 4-3-16 Yonezawa, Yamagata 992-8510, Japan
*   Correspondence: masuhara@yz.yamagata-u.ac.jp; Tel.: +81-238-26-3891

Abstract: Lead halide perovskite quantum dots (PeQDs) have excellent optical properties, such as narrow emission spectra (FWHM: 18–30 nm), a tunable bandgap (λ_{PL}: 420–780 nm), and excellent photoluminescence quantum yields (PLQYs: >90%). PeQDs are known as a material that is easily decomposed when exposed to water in the atmosphere, resulting in causing PeQDs to lower performance. On the other hand, according to the recent reports, adding water after preparing the PeQD dispersion decomposed the PeQD surface defects, resulting in improving their PLQY. Namely, controlling the amount of assisting water during the preparation of the PeQDs is a significantly critical factor to determining their optical properties and device applications. In this paper, our research group discovered the novel effects of the small amount of water to their optical properties when preparing the PeQDs. According to the TEM Images, the PeQDs particle size was clearly increased after water-assisting. In addition, XPS measurement showed that the ratio of Br/Pb achieved to be close to three. Namely, by passivating the surface defect using Ostwald ripening, the prepared PeQDs achieved a high PLQY of over 95%.

Keywords: perovskite quantum dots; light-emitting materials; water-assisted; Ostwald ripening

1. Introduction

Lead halide perovskite quantum dots (PeQDs) have excellent optical properties, such as narrow emission spectra (FWHM: 18–30 nm) [1,2], a tunable bandgap (λ_{PL}: 420–780 nm) [3,4], and excellent photoluminescence quantum yields (PLQYs: >90%) [1,5,6]. Therefore, PeQDs have been investigated and applied in a variety of fields such as light emitting diodes (LEDs) [7,8], solar cells [9,10], and photodetectors [11,12]. In general, colloidal PeQDs are synthesized by two typical liquid-phase methods, the hot injection (HI) method [3,13] and the ligand-assisted reprecipitation (LARP) method [4,14]. The HI method is the most widely used method for preparing PeQDs because it is possible to prepare size-uniform PeQDs. According to the reports by Jun et al., by using the HI method, the higher optical properties of the prepared PeQDs were achieved by the ligand exchange of dilauryldimethylammonium bromide (DDAB) [15]. In detail, DDAB works as not only the supplying sources of Br, but also the ligand, which does not detach from the PeQD surface because of the quaternary ammonium. As a result, the narrow emission spectrum and high PLQY over 71% were achieved. In addition, the LED device with the PeQDs prepared by the HI method has achieved an external quantum efficiency of 23% in a red emission [6], 22% in a green emission [16], and 12.3% in a blue emission [16]. While the prepared PeQDs with the HI

method achieves high optical properties, it is with requiring high temperatures over 100 °C and nitrogen during synthesis, resulting in its unsuitability for mass synthesis because of the high cost. On the other hand, the LARP method does not require a complicated environment to synthesize PeQDs. Therefore, not only conventional inorganic perovskites, but also organic-inorganic perovskites, could be synthesized [4,17,18]. In previous studies, various surface treatments have been applied to both inorganic and organic–inorganic perovskites by the LARP method, and the prepared PeQDs via the LARP method could achieve a high PLQY over 70%, similar to that prepared by the HI method [5,19].

The LARP method does not require a complicated environment; however, the water content of the solvent used by the synthesis of colloidal PeQDs was thoroughly controlled, with the value close to zero. In general, colloidal PeQDs are easily decomposed when they are exposed to the moisture in the atmosphere, resulting in PeQDs' decreased performance. According to previous reports [20], the effect of moisture on the structure and properties of the perovskite compound have been revealed by the simulations combined ab initio *molecular dynamics* simulations and the first-principles density functional theory. The effect of a few water molecules on the structure of the perovskite surface was simulated, resulting in the formation of hydrated compounds in a humid environment. The electronic excitation of water-absorbed perovskite tended to weaken the Pb-halogen bonds around the water molecules. This indicated that the presence of water enhanced the decomposition of the perovskite. On the other hand, there are some reports of the following: the PLQY of PeQDs were drastically improved by assisting with a little water when synthesizing. In the reports by Ying et al., a little water was added to the hexane dispersion with PeQDs to decompose the PeQD surface defects, resulting in the improvement of PLQY [21]. Namely, controlling the amount of assisting water during the preparation of the PeQDs is a significantly critical factor to determining their optical properties and device applications.

In our research, we focused on the LARP method and clarified the novel effects of the small amount of water to their optical properties when preparing the PeQDs. This method could be achieved with a high performance of the PeQDs in a one-pot preparation by assistance with water. In detail, this method, combining the phenomenon of water decomposing PeQDs and Ostwald ripening, was proposed [22]. It could be predicted that a little water could enhance the Ostwald ripening. According to the TEM Images, the PeQDs particle size was clearly increased after water-assisting. In addition, XPS measurement showed that the ratio of Br/Pb achieved to be close to three. Namely, by passivating the surface defect using Ostwald ripening, the prepared PeQDs achieved a high PLQY of over 95%.

2. Materials and Methods

2.1. Materials

$PbBr_2$ (99%) was purchased from Tokyo Chemical Industry. Hydrobromic acid (HBr 47–49%), methylamine methanol solution (MA/MeOH 40%), toluene (99.5%), 1-methyl-2-pyrrolidone (NMP 99.5%), and acetonitrile (99.5%) were purchased from Wako Pure Chemical Industries. Oleic acid (90%) and octylamine (99%) were purchased from Sigma-Aldrich. Methanol (MeOH 99.5%) and ethyl acetate (AcOEt 99.5%) were purchased from Kanto Chemical. All the materials were used without purification.

2.2. Synthesis of CH_3NH_3Br (MABr)

First, 30 mL of MA/MeOH solution was maintained at 0 °C in an ice bath and stirred for 2 h after the addition of 7 mL of HBr. After the reaction, the solvent was evaporated at a pressure of 0.1 MPa at 45 °C. The obtained white crystals were recrystallized and washed by MeOH and AcOEt and dried in a vacuum at 40 °C for 24 h.

2.3. Synthesis of Methylammonium Lead Halide ($MAPbBr_3$) PeQDs

$MAPbBr_3$ PeQDs were synthesized by the LARP method: 0.20 mmol MABr, 0.20 mmol $PbBr_2$, 15 μL of octylamine, and 18 μL of oleic acid were dissolved in 1.0 mL of NMP as a

polar solvent. Then, 250 μL of precursor solution was dropped into 4.5 mL of toluene with 0, 2.5 (0.056 vol%), 5.0 (0.11 vol%), and 7.5 (0.16 vol%) μL of water as a non-polar solvent under vigorous stirring for 10 min. To precipitate the obtained colloidal solution, acetonitrile was added at a volume ratio of 1:1, and then the mixed solutions were centrifuged at 16,500 rpm for 5 min, and the supernatants were discarded. The precipitate was dispersed in 1 mL toluene, and the solutions were centrifuged at 8000 rpm for 2 min. The dispersed supernatant was obtained and filtered through a polytetrafluoroethylene filter with a pore size 0.2 μm.

2.4. Characterization

X-ray diffraction (XRD) patterns of the samples were obtained from in-plane diffraction and were measured on a Rigaku Smart Lab (using Cu Kα radiation at 45 kV and 200 mA). The samples were observed by a JEOL JEM- 2100F transmission electron microscope (TEM) (accelerating voltage of 200 kV). The visible absorption spectra of the samples were obtained on a JASCO V-670 spectrophotometer (detecting wavelength range of 400 to 600 nm). The photoluminescence (PL) spectra and photoluminescence quantum yield (PLQY) of samples were obtained with a JASCO FP- 8600 luminescence spectrometer (exciting wavelength of 400 nm). The PL lifetime was obtained using a Hamamatsu C11367 Quantaurus-Tau. The result of the XPS measurement was obtained by using a Thermo Fisher Scientific Theta probe.

3. Results

3.1. Water-Assisted LARP Method

Figure 1 shows a schematic illustration of the water-assisted LARP method. MAPbBr$_3$ PeQDs are prepared as follows: the MAPbBr$_3$ PeQD precursor solution was injected into the mixed solvent as a non-polar solvent, which was composed of toluene and water (Figure S1). Water was completely dispersed in toluene by irradiating the ultrasound. Water is known as a solvent that decomposes MAPbBr$_3$ PeQDs. By assisting with quite a small amount of water, however, it is possible to induce Ostwald ripening, which is a phenomenon by which small sized MAPbBr$_3$ PeQDs are rapidly decomposed and redeposited on large ones [22]; finally, the surface defect of the large sized MAPbBr$_3$ PeQDs was passivated, resulting in improving their optical properties. Therefore, the difference in optical properties between the prepared MAPbBr$_3$ PeQDs without or with water are evidenced.
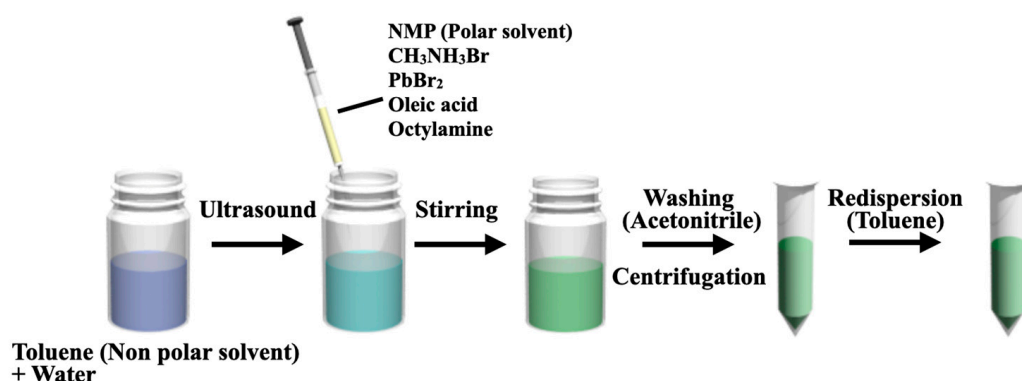

**Figure 1.** Schematic illustration of preparing MAPbBr$_3$ PeQDs by water-assisted LARP.

3.2. Ostwald Ripening of MAPbBr$_3$ PeQDs by Assisting Water

To explore the effects of water for the prepared MAPbBr$_3$ PeQDs, their morphologies were evaluated. As shown in Figures 2 and S2, the prepared MAPbBr$_3$ PeQDs with the assisted water showed larger-sized PeQDs compared to those prepared without water. Considering the MAPbBr$_3$ PeQD sizes and that their distribution value was 12.7 ± 2.8 nm (Figure 2), the mono-dispersed size and uniformity of MAPbBr$_3$ PeQDs was successfully prepared. This indicated that under assisting with a small amount of water, the small-sized

MAPbBr$_3$ PeQDs were redeposited on a large one by Ostwald ripening. This phenomenon implied that the surface defect of the large-sized MAPbBr$_3$ PeQDs was passivated by a small one, resulting in proceeding the upsizing of their particle size (Figure 3). From the distribution of the obtained particle size, it is clear that the assisting water promoted Ostwald ripening. In detail, small-sized MAPbBr$_3$ PeQDs are decomposed and redeposited on the larger MAPbBr$_3$ PeQDs. As a result, surface defects on the large sized ones were predicted to passivate by this phenomenon.
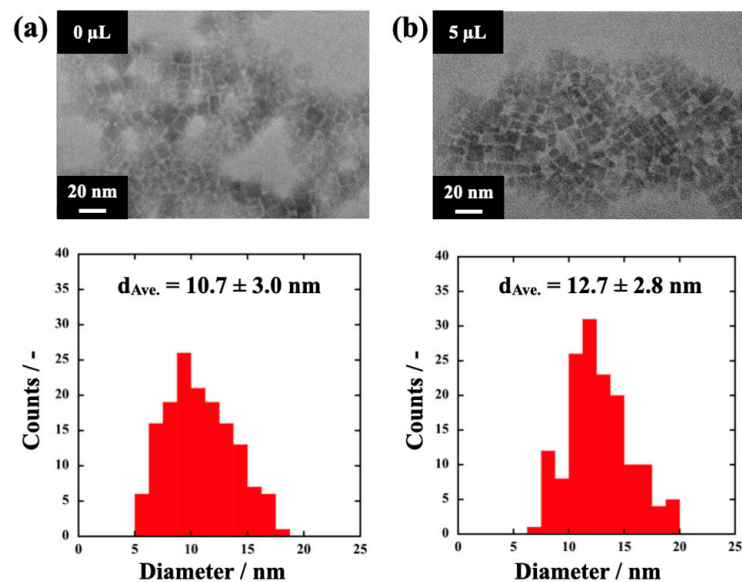
Figure 2. TEM images and size histogram of MAPbBr$_3$ PeQDs (**a**) without water and (**b**) water-assisted (5 µL).
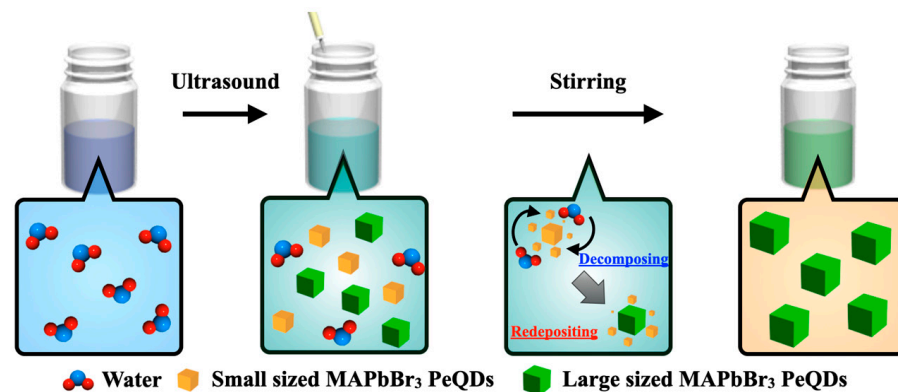
Figure 3. Schematic diagram of the phenomenon of Ostwald ripening produced by the water-assisted LARP method.

3.3. The Effect of the Assisting Water on the Prepared MAPbBr$_3$ PeQDs

To investigate the effects of the water-assisted procedure on a perovskite crystal structure on the prepared MAPbBr$_3$ PeQDs, their XRD patterns were measured. From XRD patterns, the prepared samples with between 0 vol% and 0.16 vol% of assisting water obviously show the strong peaks attributed to the (100), (110), (200), (210), (220), and (300) diffraction planes (Figures 4 and S3), which indicated a cubic perovskite crystal structure [23,24]. The XRD patterns results showed that the optimal water-assisted content will not have a negative effect on the crystal structure.
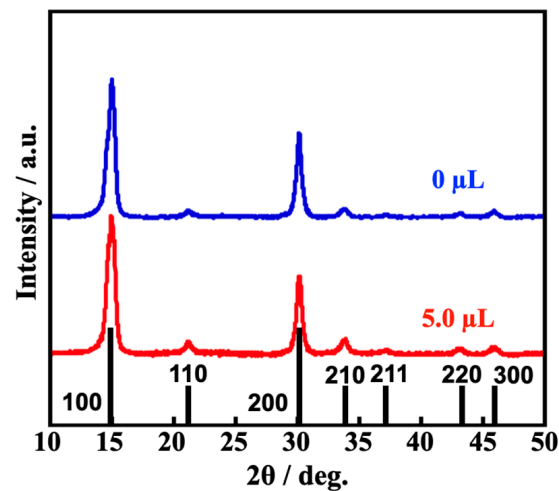
Figure 4. XRD patterns of the MAPbBr$_3$ PeQDs without water (0 μL) and water-assisted (5 μL).

Figure 5a and Figure S4a show the UV-vis absorption spectra of MAPbBr$_3$ PeQDs without and with water. As shown in the UV-vis absorption spectra, the characteristic absorption peaks of MAPbBr$_3$ PeQDs were observed. Furthermore, the absorbance of MAPbBr$_3$ PeQDs with assisted water was lower than that of MAPbBr$_3$ PeQDs without water (Figure S5). Their decrease in absorbance indicated that the number of the prepared MAPbBr$_3$ PeQDs decreased with increasing the water amount [25]. Decreasing their absorbance of the MAPbBr$_3$ PeQDs with assisted water was reasonable because the small sized MAPbBr$_3$ PeQDs was redeposited on the large one, and the total number of MAPbBr$_3$ PeQD particles was decreased. Figure 5b and Figure S4b showed the normalized PL spectra of the MAPbBr$_3$ PeQDs. The PL spectra of the prepared MAPbBr$_3$ PeQDs corresponded to the previously reported ones with cubic structures [26]. The PL peak of MAPbBr$_3$ PeQDs was red shifted from 522 nm to 526 nm by assisting with water and had a narrower FWHM compared with that of the MAPbBr$_3$ without water (Table 1). The slight red shift of the MAPbBr$_3$ PeQDs with assisting water could be implied to promote the Ostwald ripening by the addition of water [27]. As a result, their particle sizes of the prepared MAPbBr$_3$ PeQDs were uniformity, and it achieved the narrow FWHM emission [28]. In short, the PL spectra of MAPbBr$_3$ PeQDs were red shifted after the assisting of water, which clarified that their crystal growth occurred due to Ostwald ripening.
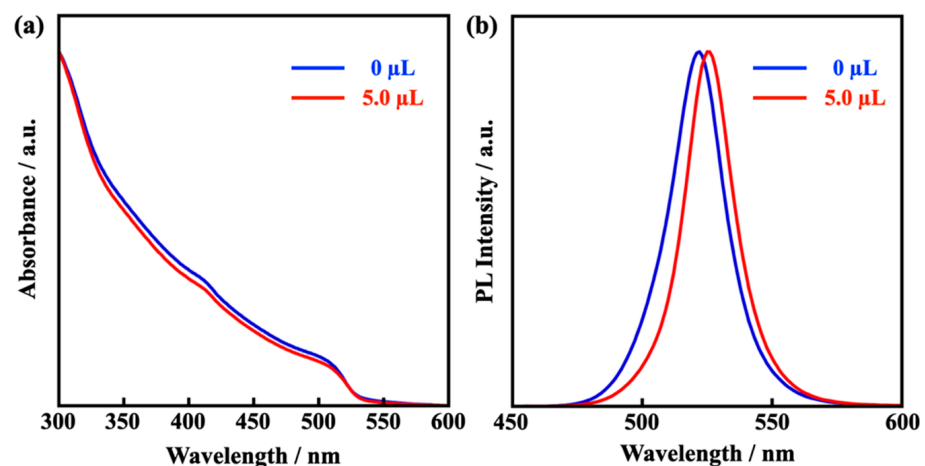

Figure 5. (**a**) UV-vis absorption spectra and (**b**) PL spectra of the MAPbBr$_3$ PeQDs without water (0 μL) and water-assisted (5 μL).

Table 1. Summary of optical properties of MAPbBr$_3$ PeQDs prepared without water (0 μL) and with water (2.5–7.5 μL).

Water-Assisted	λ_{PL}/nm	FWHM/nm	PLQY/%
0 μL	522	24.9	82.7
2.5 μL	524	23.3	91.6
5.0 μL	526	21.8	95.6
7.5 μL	524	23.0	90.4

The PLQYs of the prepared MAPbBr$_3$ PeQDs without water showed 82.7%. On the other hand, their PLQY values were increased up to 95.6% with only 5 μL assisted water (Table 1). This result implied that the optimal assisted water to prepare MAPbBr$_3$ PeQDs effectively proceeded to decompose the small-sized MAPbBr$_3$ PeQDs, resulting in passivating on the surface defects of the large sized ones by Ostwald ripening. The prepared MAPbBr$_3$ PeQDs were further investigated by time-resolved photoluminescence (Figures 6a and S6a, Table 2) to determine the charge carrier lifetime. The PL decay curve indicated that the PL lifetime of the MAPbBr$_3$ PeQDs increased to 15.4 ns with 5 μL of assisted water compared to 12.6 ns without water. From these results, the longer τ_{ave} of the prepared MAPbBr$_3$ PeQDs with assisted water of 5 μL indicates that the surface defects on the large MAPbBr$_3$ PeQDs were passivated by small MAPbBr$_3$ PeQDs as an Ostwald ripening, resulting in efficiently suppressing non-radioactive recombination by small PeQD passivation on their surface [29,30]. On the other hand, in the prepared MAPbBr$_3$ PeQDs with assisted water over 5 μL, the excess water worked to collapse MAPbBr$_3$ PeQDs because of their polarity, and it caused the increasing of MAPbBr$_3$ PeQD surface defects, resulting in a shorter τ_{ave}. From the XPS analysis, the ratio of Br/Pb showed the near unity ideal values of 2.90 on the MAPbBr$_3$ PeQDs with water compared with the value of 2.75 for that without water [31]. In addition, the Br 3d$_{5/2}$ and Br 3d$_{3/2}$ peaks on the Br 3d spectra shifted to higher binding energies by 0.1 eV, which means that Pb-Br interactions on the MAPbBr$_3$ PeQDs were stronger after assisting water (Figures 6b and S6b) [31]. It was confirmed that the surface defects of MAPbBr$_3$ PeQDs were passivated due to the longer τ_{ave} in the PL lifetime and the improvement ratio of Br/Pb by XPS measurement, which resulted in a significant improvement in PLQY. These results indicated that the water-assisted LARP method could promote the Ostwald ripening and passivate the Br defects on MAPbBr$_3$ PeQDs.
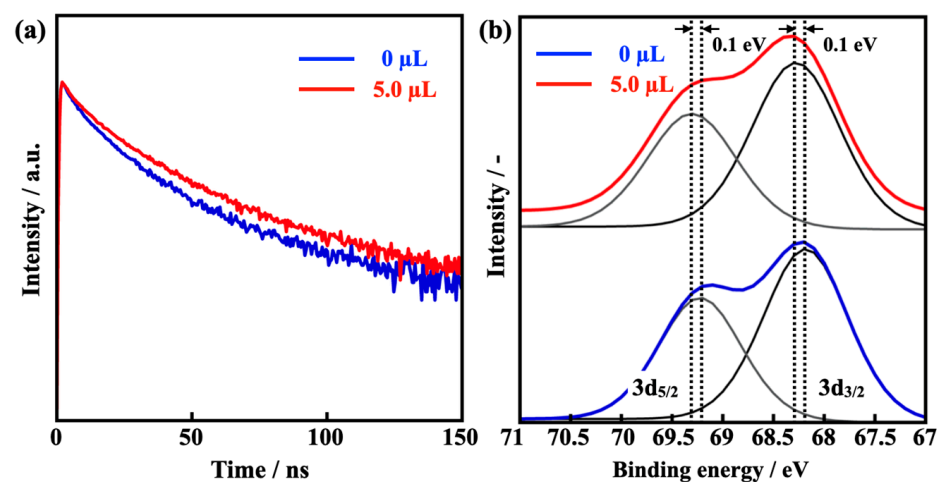
Figure 6. (**a**) PL decay curved and (**b**) XPS spectra of the MAPbBr$_3$ PeQDs without water (0 μL) and water-assisted (5 μL).

Table 2. PL decay time constant, a short-lifetime, and a long lifetime of MAPbBr$_3$ PeQDs prepared without water (0 μL) and with water (2.5–7.5 μL).

	A_1/%	A_2/%	A_3/%	τ_1/ns	τ_2/ns	τ_3/ns	$\tau_{ave.}$/ns
0 μL	50.2	44.8	5.0	3.3	10.9	29.1	12.6
2.5 μL	32.3	49.3	18.4	1.8	9.6	22.5	14.8
5.0 μL	50.2	44.1	5.7	4.1	13.3	33.4	15.4
7.5 μL	36.5	54.1	9.4	3.1	10.5	25.7	13.6

4. Conclusions

In summary, we have proposed a method to improve the performance of MAPbBr$_3$ PeQDs in one pot by a water-assisted LARP method. It was confirmed that the water-assisted LARP method promoted the Ostwald ripening process, in which small particles are dissolved and re-deposited onto larger ones. In detail, it showed that the optimal water-assisted content will not have a negative effect on their crystal structure. In addition, the PL spectra of MAPbBr$_3$ PeQDs were red shifted after being water-assisted, which clarified that their crystal growth occurred due to Ostwald ripening. Therefore, the ratio of Br/Pb was close to the ideal ratio of three after being water-assisted, resulting in a high PLQY value of over 95%. Our study provides that a one-pot method with a little water achieves high performance and elucidates the effect of water on the preparation process of MAPbBr$_3$ PeQDs.

References

1. Song, J.; Li, J.; Xu, L.; Li, J.; Zhang, F.; Han, B.; Shan, Q.; Zeng, H. Room-Temperature Triple-Ligand Surface Engineering Synergistically Boosts Ink Stability, Recombination Dynamics, and Charge Injection toward EQE-11.6% Perovskite QLEDs. *Adv. Mater.* **2018**, *30*, e1800764. [CrossRef]
2. Chen, H.; Fan, L.; Zhang, R.; Bao, C.; Zhao, H.; Xiang, W.; Liu, W.; Niu, G.; Guo, R.; Zhang, L.; et al. High-Efficiency Formamidinium Lead Bromide Perovskite Nanocrystal-Based Light-Emitting Diodes Fabricated via a Surface Defect Self-Passivation Strategy. *Adv. Opt. Mater.* **2020**, *8*, 1901390. [CrossRef]
3. Protesescu, L.; Yakunin, S.; Bodnarchuk, M.I.; Krieg, F.; Caputo, R.; Hendon, C.H.; Yang, R.X.; Walsh, A.; Kovalenko, M.V. Nanocrystals of Cesium Lead Halide Perovskites (CsPbX(3), X = Cl, Br, and I): Novel Optoelectronic Materials Showing Bright Emission with Wide Color Gamut. *Nano Lett.* **2015**, *15*, 3692–3696. [CrossRef]

4.　Zhang, F.; Zhong, H.; Chen, C.; Wu, X.-G.; Hu, X.; Huang, H.; Han, J.; Zou, B.; Dong, Y. Brightly Luminescent and Color-Tunable Colloidal CH3NH3PbX3 (X = Br, I, Cl) Quantum Dots: Potential Alternatives for Display Technology. *ACS Nano* **2015**, *9*, 4533–4542. [CrossRef]

5.　Kim, Y.-H.; Kim, S.; Kakekhani, A.; Park, J.; Park, J.; Lee, Y.-H.; Xu, H.; Nagane, S.; Wexler, R.B.; Kim, D.-H.; et al. Comprehensive defect suppression in perovskite nanocrystals for high-efficiency light-emitting diodes. *Nat. Photonics* **2021**, *15*, 148–155. [CrossRef]

6.　Wang, Y.K.; Yuan, F.; Dong, Y.; Li, J.Y.; Johnston, A.; Chen, B.; Saidaminov, M.I.; Zhou, C.; Zheng, X.; Hou, Y.; et al. All-Inorganic Quantum-Dot LEDs Based on a Phase-Stabilized alpha-CsPbI3 Perovskite. *Angew. Chem. Int. Ed. Engl.* **2021**, *60*, 2–9. [CrossRef]

7.　Huang, H.; Zhao, F.; Liu, L.; Zhang, F.; Wu, X.G.; Shi, L.; Zou, B.; Pei, Q.; Zhong, H. Emulsion Synthesis of Size-Tunable CH3NH3PbBr3 Quantum Dots: An Alternative Route toward Efficient Light-Emitting Diodes. *ACS Appl. Mater. Interfaces* **2015**, *7*, 28128–28133. [CrossRef]

8.　Ling, Y.; Yuan, Z.; Tian, Y.; Wang, X.; Wang, J.C.; Xin, Y.; Hanson, K.; Ma, B.; Gao, H. Bright Light-Emitting Diodes Based on Organometal Halide Perovskite Nanoplatelets. *Adv. Mater.* **2016**, *28*, 305–311. [CrossRef]

9.　Lee, M.M.; Teuscher, J.; Miyasaka, T.; Murakami, T.N.; Snaith, H.J. Efficient Hybrid Solar Cells Based on Meso-Superstructured Organometal Halide Perovskites. *Science* **2012**, *338*, 643–647. [CrossRef]

10.　Zhou, H.; Chen, Q.; Li, G.; Luo, S.; Song, T.; Duan, H.; Hong, Z.; You, J.; Liu, Y.; Yang, Y. Interface engineering of highly efficient perovskite solar cells. *Science* **2014**, *345*, 542–546. [CrossRef]

11.　Jang, D.M.; Park, K.; Kim, D.H.; Park, J.; Shojaei, F.; Kang, H.S.; Ahn, J.P.; Lee, J.W.; Song, J.K. Reversible Halide Exchange Reaction of Organometal Trihalide Perovskite Colloidal Nanocrystals for Full-Range Band Gap Tuning. *Nano Lett.* **2015**, *15*, 5191–5199. [CrossRef]

12.　Jang, D.M.; Kim, D.H.; Park, K.; Park, J.; Lee, J.W.; Song, J.K. Ultrasound synthesis of lead halide perovskite nanocrystals. *J. Mater. Chem. C* **2016**, *4*, 10625–10629. [CrossRef]

13.　Zheng, W.; Wan, Q.; Zhang, Q.; Liu, M.; Zhang, C.; Wang, B.; Kong, L.; Li, L. High-efficiency perovskite nanocrystal light-emitting diodes via decorating NiOx on the nanocrystal surface. *Nanoscale* **2020**, *12*, 8711–8719. [CrossRef]

14.　Yan, F.; Xing, J.; Xing, G.; Quan, L.; Tan, S.T.; Zhao, J.; Su, R.; Zhang, L.; Chen, S.; Zhao, Y.; et al. Highly Efficient Visible Colloidal Lead-Halide Perovskite Nanocrystal Light-Emitting Diodes. *Nano Lett.* **2018**, *18*, 3157–3164. [CrossRef] [PubMed]

15.　Pan, J.; Quan, L.N.; Zhao, Y.; Peng, W.; Murali, B.; Sarmah, S.P.; Yuan, M.; Sinatra, L.; Alyami, N.M.; Liu, J.; et al. Highly Efficient Perovskite-Quantum-Dot Light-Emitting Diodes by Surface Engineering. *Adv. Mater.* **2016**, *28*, 8718–8725. [CrossRef] [PubMed]

16.　Dong, Y.; Wang, Y.K.; Yuan, F.; Johnston, A.; Liu, Y.; Ma, D.; Choi, M.J.; Chen, B.; Chekini, M.; Baek, S.W.; et al. Bipolar-shell resurfacing for blue LEDs based on strongly confined perovskite quantum dots. *Nat. Nanotechnol.* **2020**, *15*, 668–674. [CrossRef] [PubMed]

17.　Chin, X.Y.; Perumal, A.; Bruno, A.; Yantara, N.; Veldhuis, S.A.; Martínez-Sarti, L.; Chandran, B.; Chirvony, V.; Lo, A.S.-Z.; So, J.; et al. Self-assembled hierarchical nanostructured perovskites enable highly efficient LEDs via an energy cascade. *Energy Environ. Sci.* **2018**, *11*, 1770–1778. [CrossRef]

18.　Zirak, M.; Moyen, E.; Alehdaghi, H.; Kanwat, A.; Choi, W.-C.; Jang, J. Anion- and Cation-Codoped All-Inorganic Blue-Emitting Perovskite Quantum Dots for Light-Emitting Diodes. *ACS Appl. Nano Mater.* **2019**, *2*, 5655–5662. [CrossRef]

19.　Zhao, H.; Chen, H.; Bai, S.; Kuang, C.; Luo, X.; Teng, P.; Yin, C.; Zeng, P.; Hou, L.; Yang, Y.; et al. High-Brightness Perovskite Light-Emitting Diodes Based on FAPbBr3 Nanocrystals with Rationally Designed Aromatic Ligands. *ACS Energy Lett.* **2021**, *6*, 2395–2403. [CrossRef]

20.　Zhang, L.; Ju, M.G.; Liang, W. The effect of moisture on the structures and properties of lead halide perovskites: A first-principles theoretical investigation. *Phys. Chem. Chem. Phys.* **2016**, *18*, 23174–23183. [CrossRef]

21.　Liu, Y.; Li, F.; Liu, Q.; Xia, Z. Synergetic Effect of Postsynthetic Water Treatment on the Enhanced Photoluminescence and Stability of CsPbX3 (X = Cl, Br, I) Perovskite Nanocrystals. *Chem. Mater.* **2018**, *30*, 6922–6929. [CrossRef]

22.　Umemoto, K.; Takeda, M.; Tezuka, Y.; Chiba, T.; White, M.S.; Inose, T.; Yoshida, T.; Asakura, S.; Toyouchi, S.; Uji-i, H.; et al. Separation of mono-dispersed CH3NH3PbBr3 perovskite quantum dots via dissolution of nanocrystals. *CrystEngComm* **2018**, *20*, 7053–7057. [CrossRef]

23.　Shi, D.; Adinolfi, V.; Comin, R.; Yuan, M.; Alarousu, E.; Buin, A.; Chen, Y.; Hoogland, S.; Rothenberger, A.; Katsiev, K.; et al. Low trap-state density and long carrier diffusion in organolead trihalide perovskite single crystals. *Science* **2015**, *347*, 519–522. [CrossRef] [PubMed]

24.　Yang, H.S.; Noh, S.H.; Suh, E.H.; Jung, J.; Oh, J.G.; Lee, K.H.; Jang, J. Enhanced Stabilities and Production Yields of MAPbBr3 Quantum Dots and Their Applications as Stretchable and Self-Healable Color Filters. *ACS Appl. Mater. Interfaces* **2021**, *13*, 4374–4384. [CrossRef]

25.　De Geyter, B.; Hens, Z. The absorption coefficient of PbSe/CdSe core/shell colloidal quantum dots. *Appl. Phys. Lett.* **2010**, *97*, 161908. [CrossRef]

26.　Woo Choi, J.; Woo, H.C.; Huang, X.; Jung, W.G.; Kim, B.J.; Jeon, S.W.; Yim, S.Y.; Lee, J.S.; Lee, C.L. Organic-inorganic hybrid perovskite quantum dots with high PLQY and enhanced carrier mobility through crystallinity control by solvent engineering and solid-state ligand exchange. *Nanoscale* **2018**, *10*, 13356–13367. [CrossRef]

27.　Sichert, J.A.; Tong, Y.; Mutz, N.; Vollmer, M.; Fischer, S.; Milowska, K.Z.; Garcia Cortadella, R.; Nickel, B.; Cardenas-Daw, C.; Stolarczyk, J.K.; et al. Quantum Size Effect in Organometal Halide Perovskite Nanoplatelets. *Nano Lett.* **2015**, *15*, 6521–6527. [CrossRef]

28. Shao, H.; Bai, X.; Pan, G.; Cui, H.; Zhu, J.; Zhai, Y.; Liu, J.; Dong, B.; Xu, L.; Song, H. Highly efficient and stable blue-emitting CsPbBr3@SiO2 nanospheres through low temperature synthesis for nanoprinting and WLED. *Nanotechnology* **2018**, *29*, 285706. [CrossRef]

29. Zhang, C.; Wang, S.; Li, X.; Yuan, M.; Turyanska, L.; Yang, X. Core/Shell Perovskite Nanocrystals: Synthesis of Highly Efficient and Environmentally Stable $FAPbBr_3$/CsPbBr3 for LED Applications. *Adv. Funct. Mater.* **2020**, *30*, 1910582. [CrossRef]

30. Lee, H.B.; Kumar, N.; Tyagi, B.; Ko, K.-J.; Kang, J.-W. Dimensionality and Defect Engineering Using Fluoroaromatic Cations for Efficiency and Stability Enhancement in 3D/2D Perovskite Photovoltaics. *Solar RRL* **2020**, *5*, 2000589. [CrossRef]

31. He, S.; Kumar, N.; Beng Lee, H.; Ko, K.-J.; Jung, Y.-J.; Kim, J.-I.; Bae, S.; Lee, J.-H.; Kang, J.-W. Tailoring the refractive index and surface defects of CsPbBr3 quantum dots via alkyl cation-engineering for efficient perovskite light-emitting diodes. *Chem. Eng. J.* **2021**, *425*, 130678. [CrossRef]